coatings

MDPI

Article

Study on Durability and Dynamic Deicing Performance of Elastomeric Coatings on Wind Turbine Blades

Ke Li [1,†], Zhiliang Xue [2,*,†], Danqing Jiang [3], Zhichun Chen [4], Qi Si [3], Jixin Liu [3] and Yonggang Zhou [2]

[1] Department of Energy and Environment System Engineering, Zhejiang University of Science and Technology, Hangzhou 310023, China; 118011@zust.edu.cn
[2] State Key Laboratory of Clean Energy Utilization, Zhejiang University, Hangzhou 310027, China; trooper@zju.edu.cn
[3] Guodian Ningbo Wind Power Development Co., Ltd., Ningbo 315000, China; 12056750@ceic.com (D.J.); qi.si@ceic.com (Q.S.); 12023321@ceic.com (J.L.)
[4] Department of Chemistry, Zhejiang University, Hangzhou 310027, China; czc9966@163.com
* Correspondence: xuezhiliang@zju.edu.cn
† These authors contributed equally to this work.

Abstract: Durable elastomeric deicing coatings were developed for the anti-icing and deicing of wind turbine blades in this study. Our developed deicing coatings demonstrated extremely low ice adhesion strength (~15 kPa). Silica was added to enhance the icephobic surfaces' durability. The life of the deicing coating with silica was extended by 1.2 times. After 168 h of xenon lamp irradiation, there were no significant changes in the chemical composition of the coatings. Due to the increasing roughness and the decreasing tensile modulus, the contact angle of the aged coatings decreased by 14°. Further outdoor research was carried out on a wind farm for two months to investigate the influence of natural insolation and wind erosion on the elastic deicing coatings. The aged coating still maintained a high hydrophobicity and low ice adhesion strength. The contact angle stabilized at 107°, and the ice adhesion strength was 75% lower than that of the uncoated wind turbine blade. The elastomeric deicing coatings had three advantages: a lagging freezing time, low ice accumulation, and a short icing/deicing cycle. The results of field experiments on the naturally aged coatings showed that the freezing time of the coated blade was delayed by 20 min, and the ice on the coated blade was 29% thinner than that on the uncoated blade.

Keywords: elastic deicing coating; aging; wind turbine blade; field experiment; dynamic deicing performance

Citation: Li, K.; Xue, Z.; Jiang, D.; Chen, Z.; Si, Q.; Liu, J.; Zhou, Y. Study on Durability and Dynamic Deicing Performance of Elastomeric Coatings on Wind Turbine Blades. *Coatings* **2024**, *14*, 870. https://doi.org/10.3390/coatings14070870

Academic Editor: Muhammad Ahsan Bashir

Received: 4 June 2024
Revised: 4 July 2024
Accepted: 5 July 2024
Published: 11 July 2024

1. Introduction

As a clean and renewable energy source, wind power is one of the fastest-growing industries, and it has become the third largest power resource in China after coal and water. Many wind farms are located in cold regions or at high altitudes, but low temperatures increase the possibility of icing events. Icing on wind turbine blades may cause many operational problems, such as power losses, mechanical failures, and safety hazards [1]. In order to address the icing challenge and reduce the frequency of unscheduled shutdowns and maintenance issues caused by icing, many active and passive anti- and deicing methods have been tried. Icing mitigation technology mainly includes thermal, mechanical, and chemical deicing. Most active deicing technologies require intensive maintenance and a high energy input and pose safety hazards, such as the attraction of lightning [2]. Anti-icing coatings are low-cost, do not require special lightning protection, and enable easy blade maintenance [3]. Therefore, a range of deicing coatings have been developed, including superhydrophobic, liquid-infused, and hydrated surfaces [4]. Among a wide range of icephobic surfaces, elastomers have shown minimum ice adhesion and can achieve exceptional anti-icing properties [5,6].

Strong hydrophobic properties, low surface energy, and a tunable modulus make silicone rubber perform well as an anti-icing material [7–10]. Darryl et al. [11] developed a polydimethylsiloxane (PDMS) coating with ultra-low adhesion to ice. Due to its deformability, the ice detachment from PDMS is localized rather than monolithic, which greatly reduces the shear force required for deicing. Under sufficient tensile stress, ice locally detaches from the PDMS gel surface but soon reattaches through van der Waals forces and traps air cavities at the interface. Air cavities propagate in a separation pulse and result in a stick–slip motion and a low ice adhesion strength. The ice adhesion strength can be further decreased by introducing internal holes into PDMS, enlarging the internal holes, and increasing the number of layers with internal holes [12]. Irajizad et al. [6] reported a new physical concept called stress localization and corresponding icephobic elastomers. These materials utilized the stress-localization function to induce cracks at the ice–material interface and consequently minimized ice adhesion to 1 kPa. Silica aerogels, hydrophobic fumed silica nanoparticles, micro-fibers, and nanoparticles were added to elastic icephobic coatings to enhance their hydrophobicity, mechanical strength, and durability [13–16]. Many studies have tested the durability of elastic icephobic coatings under different conditions, such as icing/deicing cycles, erosion by acidic and basic chemical solutions, UV radiation, sandblasting, abrasion cycles, and liquid flow impingement [6,11,17–19]. However, limited efforts have been dedicated to elastic coatings' durability and capability to maintain icephobic performance in real wind power plant environments [16].

In this study, we developed durable deicing coatings made of viscoelastic, non-toxic, non-corrosive, nonflammable, inert, and inexpensive silicone rubber. Hydrophobic silica nanoparticles were added to enhance the durability of the coatings. The aging mechanism of some coatings was determined under simulated insolation. The other coatings were subjected to natural insolation and wind erosion on a wind farm to figure out the aging calendar. The deicing performance of the coatings after one month of natural aging was verified using dynamic analysis in the field. The aging of the elastic deicing coatings was studied at full size, from the laboratory to the field, which has rarely been reported in previous research. In the previous studies on deicing coatings, the deicing performance has mainly been evaluated via a static process. However, the actual stress state of ice on wind turbine blades is complicated. During blade rotation, the ice on wind turbine blades is subjected to a periodic tangential force resulting from wind and gravity. Here, the dynamic deicing performance of the elastic coatings was verified using a small wind turbine on a real wind farm. The results preliminarily verified the feasibility of elastic deicing coatings on a real wind turbine.

2. Materials and Methods

2.1. Preparation of Elastic Deicing Coatings and Performance Test

The procedure for the development of the elastic deicing coatings was as follows: First, hydrophobic silica (SiO_2, purchased from Jinan Zhiding Co., Ltd., Jinan, China) was dissolved in hexamethyldisiloxane (HMDSO, purchased from Shanghai Macklin Biochemical Technology Co., Ltd., Shanghai, China) and then stirred mechanically for 5 min. The diameter of the silica was 20 nm. The silica/HMDSO dispersions were filtered using a 200-mesh filter cloth. Second, silicone rubber (SR, RTV neutral cure sealant, Dow Corning Corporation, Midland, MI, USA) was added to HMDSO, and the mixture was stirred for 20 min. The filtered silica/HMDSO dispersions were slowly poured into the HMDSO/SR mixture and stirred for 10 min. The HMDSO/SR ratios of the HMDSO/SR/silica mixtures were 2:1 and 4:1 (by weight). The silica proportions of the mixture were 0.125%, 0.25%, 0.5%, 1%, and 2% (by weight). The prepared elastic deicing coatings were brush-painted onto blade samples cut from a real wind turbine blade.

A horizontal shear test was used for determining the ice adhesion strength in this study [20]. A schematic of the experiments is shown in Figure 1. The coated and uncoated blade samples were placed on the top of a semiconductor cooling plate. The temperature of the cooling plate was kept at -18 ± 0.1 °C and monitored using a thermocouple on top

of the cooling plate. The test ice was produced by freezing water in a square acrylic cuvette that was 10 mm by 10 mm. The ice adhesion strength was measured with a force transducer (SF-100) by pulling on the side of the ice molds at a constant velocity. The average of at least 5 readings was taken for each sample. The ice adhesion strength was defined as the ratio of the peak removal force F to the interface area of the ice [5].

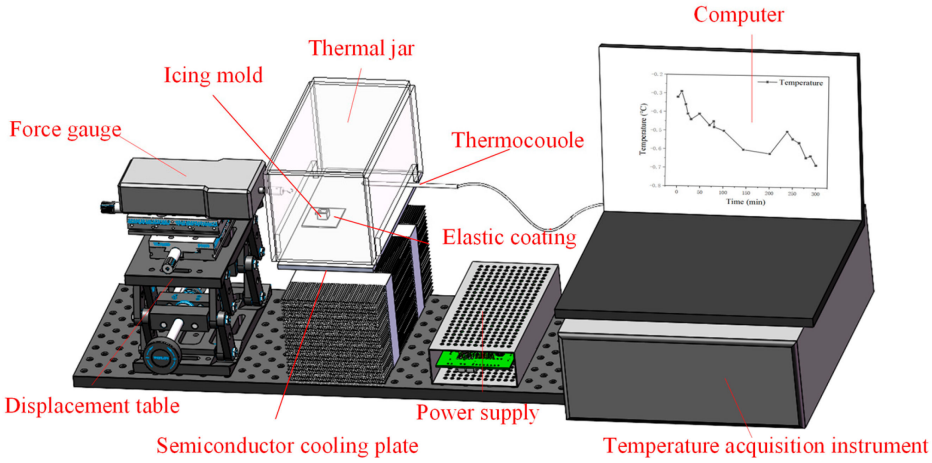

Figure 1. Horizontal shear test apparatus for ice adhesion.

The static water contact angle (CA) of the elastic deicing coatings was measured with a video contact angle measurement system (OCA20, DataPhysics Instruments GmbH, Filderstadt, Germany) using 3.5 µg droplets of deionized water. The average of at least 3 contact angle readings was taken for each sample. The surface morphology of the elastic deicing coating was investigated using a field-emission scanning electron microscope (SEM, Hitachi SU3500, Hitachi, Ltd., Tokyo, Japan). The SEM pictures with a magnification ranging from 500 to 10,000 times were compared (Figure S1). The pictures with a magnification of 1000 times, which have the highest resolution and relatively more information, were studied.

In order to determine the effect of silica on the durability of the elastic deicing coatings, a wind fan was installed on the roof of the lab (Figure S2). The fan was propelled by a three-phase asynchronous motor, and the speed of the fan was controlled at 0–300 r/min using a frequency converter. The elastic deicing coatings with and without silica were painted on two different blades of the fan. The HMDSO/SR ratio of the coatings was 2:1, and the silica proportion was 0.25%. The fan was operated continuously outdoors for 150 days.

2.2. Accelerated Aging of Elastic Deicing Coatings using Xenon Lamp

The accelerated aging tests on the elastic deicing coatings were operated under a xenon lamp. The coating samples were prepared according to the procedure in Section 2.1. The HMDSO/SR ratio of the coatings was 4:1, and the silica content was 0.25% (by weight). The coatings were spray-painted on a 10 cm-by-10 cm square sample of tempered glass and dried for 24 h at room temperature. This step was repeated 20 times. The coatings peeled from the glass were used for accelerated aging tests in a xenon lamp light-accelerated aging test chamber (Q-SUN Xe-3-HDSE, Q-lab cooperation, Westlake, OH, USA). The xenon lamp aging test was operated according to standard GB/T16422.2-2022. The test temperature was 65 °C, and the humidity was 50% RH. The power output was 0.51 W/m^2. The dry and wet cycles lasted for 102 min and 18 min. The accelerated aging experiment lasted 168 h, and the physicochemical properties of the coatings at different times were tested. Many coating samples were placed in the accelerated aging test chamber first. Then, 4 pieces were taken at each testing time to measure the chemical structure, contact angle, surface morphology, and mechanical properties. Due to the irreversible damage caused by testing, the tested samples were not put back into the chamber for more tests. The chemical structure of the elastic deicing coatings was determined using Fourier-transform infrared

(FTIR) spectroscopy (Nicolet iS50, Thermo Fisher Scientific Inc., Waltham, MA, USA). The surface morphology of the coatings was investigated using SEM. The mechanical properties of the deicing coatings were measured according to GB/T 528-2009 using a universal testing machine (CMT4304, MTS Corp, Eden Prairie, MN, USA) in stretching mode.

2.3. Natural Aging Properties of Elastic Deicing Coatings

A natural aging test of the elastic deicing coatings was performed on a wind farm located 800 m high in the mountains. During the test period, the wind farm was subjected to cold waves 5 times, and 1.57 million kilowatt-hours were lost due to the blades icing over. The maximum wind speed was 12.29 m/s, and the minimum temperature was −8 °C (Figure 2). The elastic deicing coatings were painted on two blades located in different areas with sufficient wind and light. Then, silicone papers were stuck onto the coatings. On the top of the silicone papers, the elastic deicing coatings were painted again for testing (Figure 3). The HMDSO/SR/SiO_2 ratio of the deicing coatings was 2:1:0.0075. The silicone papers covered with coatings were cut into squares measuring 50 mm by 50 mm. One square sample was collected every half month to measure the contact angle, ice adhesion strength, and surface microstructure.

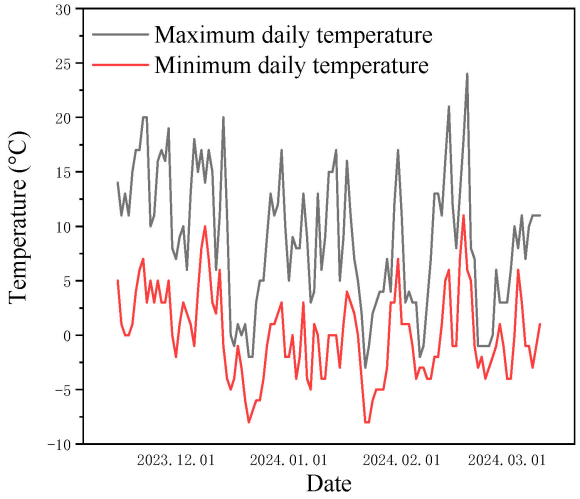

Figure 2. The daily temperature at the wind farm during the test period.

Figure 3. Blades on wind farm used for natural wind erosion and insolation aging tests.

2.4. Dynamic Deicing Test on Wind Farm

The dynamic deicing test was performed on a mountaintop, where the wind direction and intensity were relatively steady (Figure S3). The rated power of the experimental small wind turbine was 300 W. The blades of the small wind turbine were made of a glass fiber

composite, and the blades were 1 m in length. The fan blade was marked with a line every 10 cm from tip to root. One of the three blades was coated with an elastic deicing coating, and the HMDSO/SR/SiO_2 ratio of the coating was 2:1:0.0075. During the experiment, the temperature was −5–0 °C, the humidity was above 90%, and the highest wind speed was 37.6 m/s. According to the icing situation, the rotating wind turbine was stopped manually, and pictures were taken. With the plotting scale previously marked on the blade, the ice thickness was measured and calculated using the Image J analyzer (Figure S4).

3. Results

3.1. Effect of Silica on the Durability of Elastic Deicing Coatings

To make the elastic deicing coatings, HMDSO was used to dilute SR to make it easier to brush (HMDSO/SR = 2:1) or spray (HMDSO/SR = 4:1). As the amount of HMDSO increased, the ice adhesion strength increased by about 25%, which might be due to the lower water contact angle and increased surface roughness. Silica could have slightly decreased the ice adhesion strength. As the silica content of the coatings increased from 0.25% to 2%, the ice adhesion strength increased from 22 kPa to 28 kPa (HMDSO/SR = 2:1) (Figure 4a). However, the contact angle (at 112°–118°) of the coating surface remained constant as the amount of silica nanoparticles increased from 0.125 to 2% (Figure 4b). It has been proved that a low silica content has a limited effect on the contact angle [21]. The hydrophobicity and ice adhesion strength of the deicing coatings were largely related to the surface morphology [22]. As shown in Figure 5, the surfaces of the deicing coatings with an HMDSO/SR ratio of 2:1 were much smoother than those of the coatings with an HMDSO/SR ratio of 4:1. Our previous research showed that most of the HMDSO evaporated during coating curing. In the coatings with a higher HMDSO/SR ratio, mass HMDSO evaporation might result in surface undulation and silica agglomeration. The silica was dispersed in the elastic deicing coatings when the content was less than 1%, but more silica particles agglomerated when the silica content increased to 2%. The agglomerated silica particles were exposed on the surface of the coatings with a higher HMDSO ratio (Figure 5j), while most particles were buried in the coatings with a lower HMDSO ratio (Figure 5e). Using an increasing amount of silica made the surfaces significantly rougher and enabled mechanical interlocking between the ice and coatings, thus facilitating ice adhesion [23]. In addition, the shear force required to separate ice from an elastomeric coating depends on the Young's modulus, which might be affected by the filler volume fraction of nanoparticles [24,25].

The low ice adhesion strength of elastic deicing coatings is highly dependent on their elasticity, but high elasticity leads to poor mechanical properties and unsatisfactory erosion resistance [25,26]. Nano-silica precipitation can improve the mechanical properties of elastomers [27,28]. Here, elastic deicing coatings with and without silica were painted on a small wind turbine, which was operated outdoors for 150 days. During the first 90 days, even though many dust particles attached to the coatings both with and without silica, the coatings were intact (Figure 6). After 126 days of operation, the tip of the blade coated without silica was torn because of the high linear velocity this area is exposed to. Meanwhile, more ice accumulated in this place during icing. A coating failure in this position would significantly reduce the anti-icing performance of the coatings. However, after 150 days of operation, the coating with silica was still intact. This indicates that using silica extended the life of the coating by at least 20%. In order to verify the deicing performance of the coatings after long-term operation and identify how they age, further research was conducted on deicing coatings with silica.

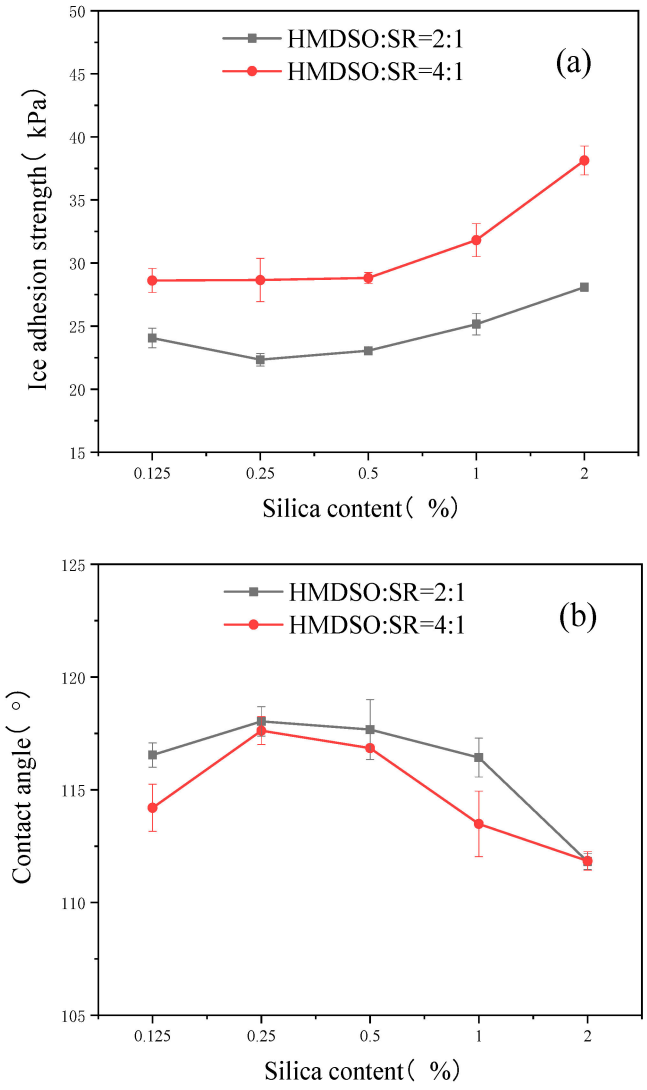

Figure 4. Effect of silica nanoparticle participation on ice adhesion strength (**a**) and contact angle (**b**) of elastic deicing coatings.

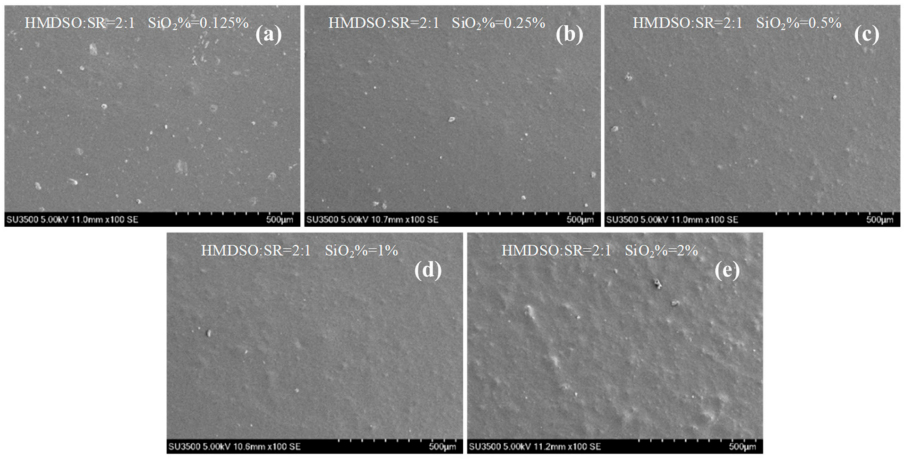

Figure 5. *Cont.*

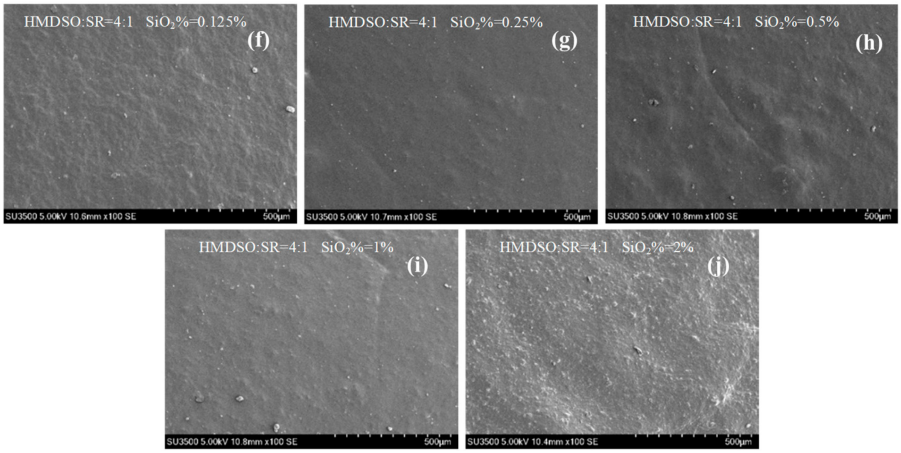

Figure 5. SEM images of elastic deicing coatings with different silica ratios,(**a**)HMDSO/SR = 2:1, SiO_2% = 0.125%; (**b**) HMDSO/SR = 2:1, SiO_2% = 0.25%; (**c**) HMDSO/SR = 2:1, SiO_2% = 0.5%; (**d**) HMDSO/SR = 2:1, SiO_2% = 1%; (**e**) HMDSO/SR = 2:1, SiO_2% = 2%; (**f**) HMDSO/SR = 4:1, SiO_2% = 0.125%; (**g**) HMDSO/SR = 4:1, SiO_2% = 0.25%; (**h**) HMDSO/SR = 4:1, SiO_2% = 0.5%; (**i**) HMDSO/SR = 4:1, SiO_2% = 1%; (**j**) HMDSO/SR = 4:1, SiO_2% = 2%.

Figure 6. Outdoor aging behavior of elastic deicing coatings with and without silica.

3.2. Xenon Lamp Accelerated Aging of Elastic Deicing Coatings

Accelerated aging tests on the elastic deicing coatings were carried out under a xenon lamp. After 90 h of xenon lamp irradiation, the contact angle of the elastic deicing coatings decreased from 129° to 115° and remained stable for the following 78 h (Figure 7). The main chain of silicone rubber is mainly composed of a silica network, and silicon and oxygen atoms are alternately arranged on the main chain. Non-polar methyl groups are closely arranged on both sides of the main chain and oriented towards the surface, thus making silicone rubber strongly hydrophobic [29]. The FTIR results of the deicing coatings at different times are shown in Figure 8. There were pronounced bands appearing at 2963 cm^{-1}, 1260 cm^{-1}, 1090 cm^{-1}, 1020 cm^{-1}, and 799 cm^{-1}, which were assigned to CH_3 stretching, CH_3 deformation, Si-O stretching, and the Si-O-Si groups, respectively [30]. As shown in Figure 8b, a smaller quantity was transmitted at 2963 cm^{-1} and 1260 cm^{-1} for the aged coatings than for the new coatings. This indicates that the decreasing contact angle of the aged coatings might be due to the decreasing quantity of methyl groups. The increasing transmittance of Si-O indicates a cross-linking reaction on the main chain, thus enhancing the polarity of the coatings and inhibiting hydrophobicity. Many researchers have shown that the surface roughness of aged silicone rubber increases with time, resulting in low hydrophobicity [10,31–33]. In this study, the SEM pictures of the deicing coatings show that both the new and aged coatings had dense surfaces (Figure 9). After 120 h of irradiation, the surface became rough, and the white granules appeared on the surface, which might be due to silicon leakage from the coating. The xenon lamp spectrum, which is concentrated in the

visible region, had enough energy to break the Si-C bonds and lead to Si precipitation from the deicing coatings. The tensile modulus of the elastic deicing coatings decreased from 1.62 MPa to 1.27 MPa after 50 h of irradiation. During the following 70 h, the tensile modulus remained stable and then decreased to 0.88 MPa in the last 40 h (Figure 10). Given that the changes in contact angle and chemical construction were not remarkable, the changes in surface microtopography and elasticity might be the main reasons for deicing performance degeneration.

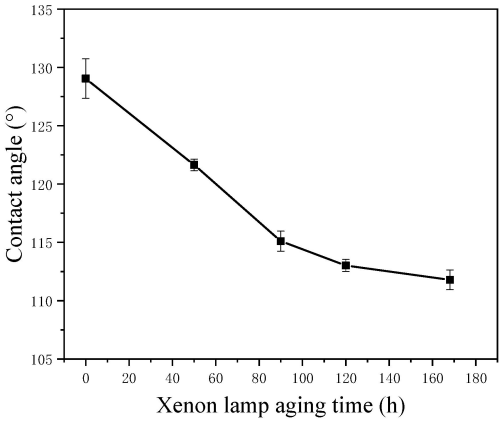

Figure 7. Xenon lamp irradiation aging effect on contact angle of elastic deicing coatings.

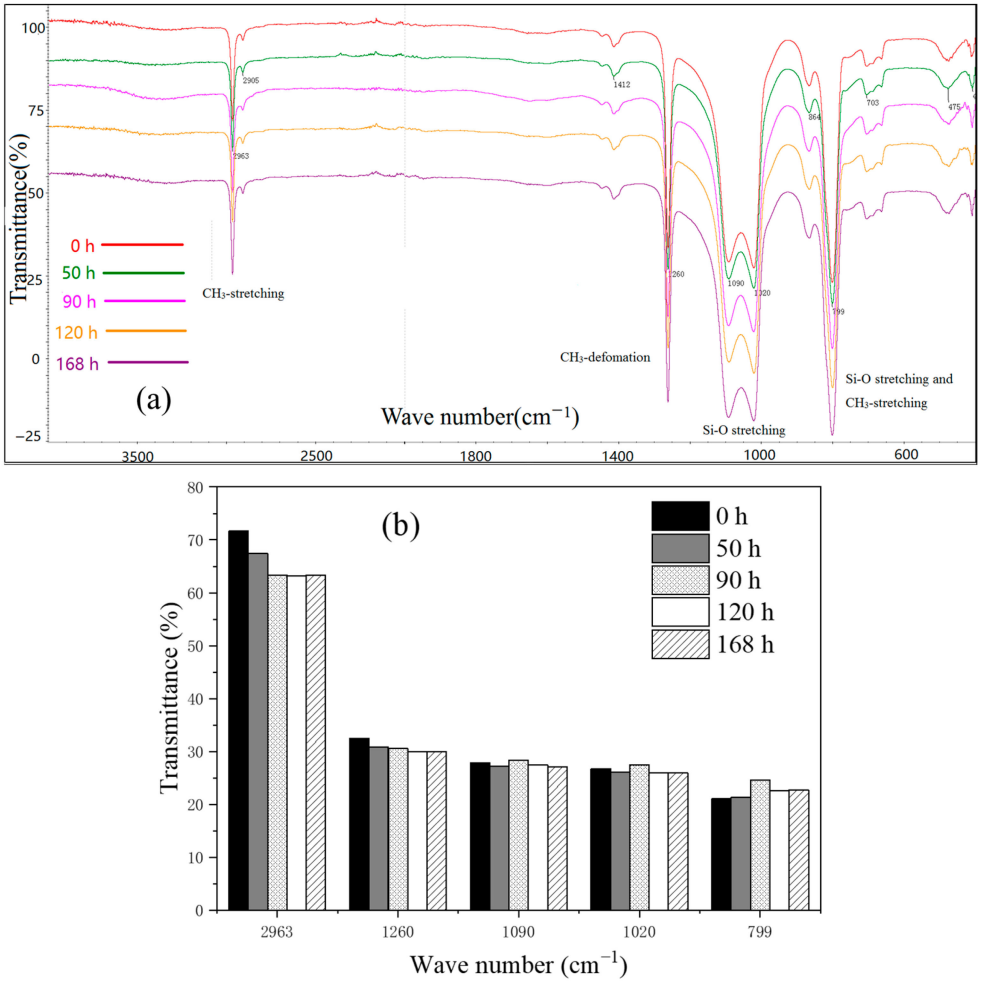

Figure 8. FTIR spectra of the elastic deicing coatings at different times: (**a**) FTIR spectra; (**b**) transmittance at some specific wave numbers.

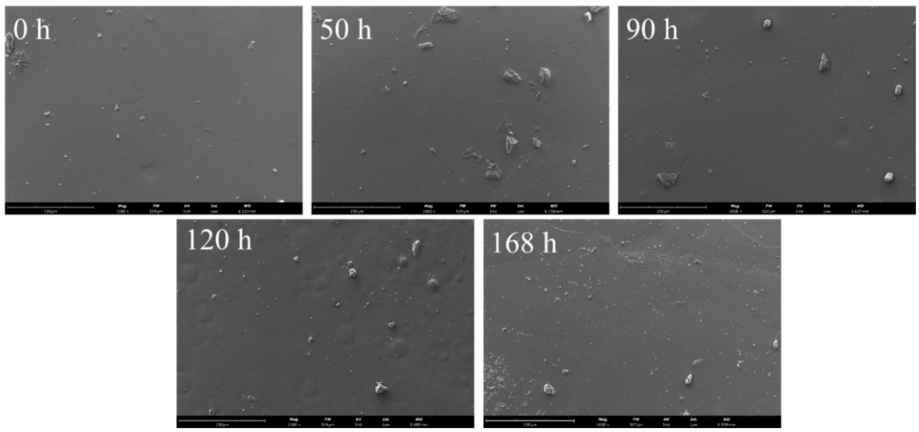

Figure 9. SEM images of elastic deicing coatings at different times.

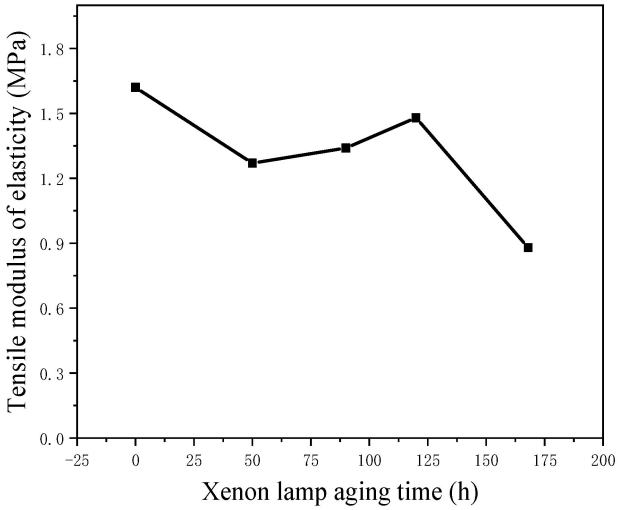

Figure 10. Xenon lamp irradiation aging effect on tensile modulus of elastic deicing coatings.

3.3. Natural Aging of Coatings on Wind Farm

After two months of insolation and wind erosion, the ice adhesion strength of the elastic coatings was higher than that of the non-aged coatings. Within one month, the ice adhesion of the coatings increased from 15 kPa to 70 kPa, and the adhesion then remained stable during the second month (Figure 11a). The water contact angle significantly decreased for 60 days and then remained stable. The contact angle of the insolated coatings decreased from 119° to 107°, and the contact angle of the wind-eroded coatings decreased to 110° (Figure 11b). After exposure to insolation and wind erosion, more dust granules were attached to the surface of the coatings (Figure 12). Interestingly, less dust attached to the coatings under wind erosion than to those under insolation, which might be due to the wind blowing it away. Thus, the contact angle of the coatings under wind erosion was higher than that of the coatings under insolation. As observed for the aged coatings under xenon lamp irradiation, many white granules appeared on the aged coatings under insolation and wind erosion. Both insolation and wind erosion increased the roughness of the elastic coatings, and greater roughness allows for surfaces with a higher surface tension to be wetted more easily by liquids [34,35]. Even though the anti-icing performance degraded due to insolation and wind erosion, the ice adhesion of the aged coatings was still below 100 kPa, and they could be classified as icephobic surfaces [36]. The ice adhesion of the aged coatings was about 75% lower than that of the uncoated wind turbine blade. This demonstrates the application feasibility of elastic coatings on wind turbine blades. Further research was conducted to verify the dynamic deicing performance of one-month-old coatings on wind turbine blades.

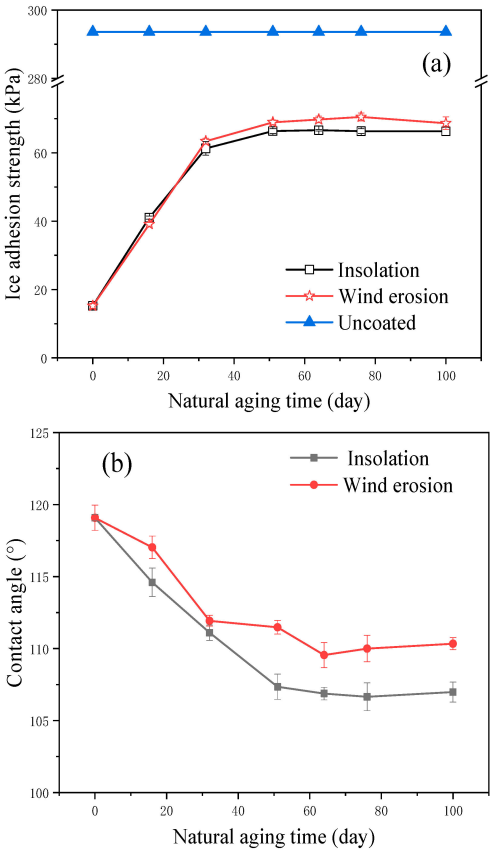

Figure 11. Natural insolation and wind erosion effects on ice adhesion strength (**a**) and contact angle (**b**) of elastic deicing coatings.

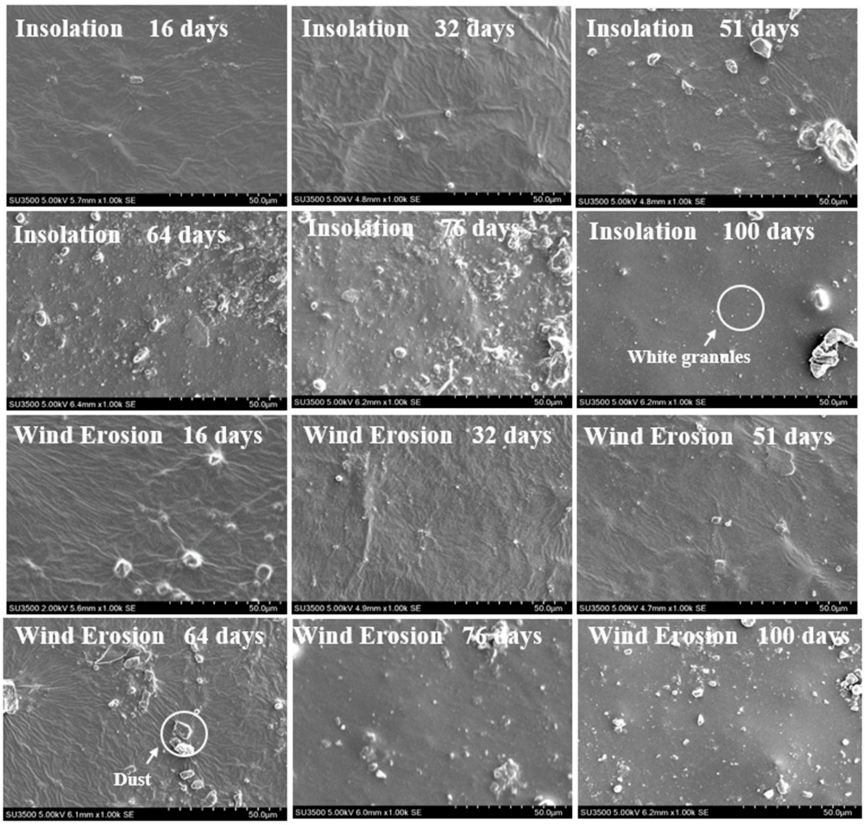

Figure 12. SEM images of insolated and wind-eroded elastic deicing coatings at different times.

3.4. Dynamic Deicing Performance of Elastic Coatings on Wind Farm

The dynamic deicing performance of the elastic deicing coatings was tested on a small wind turbine. The elastic deicing coatings were painted on the blade, and then the wind turbine was operated on a wind farm for one month before being tested. The results show that the elastic deicing coatings delayed freezing, reduced the ice adhesion strength, and reduced the icing mass. Like on a real wind turbine, the amount of ice linearly increased from the root to the tip and mainly accumulated at the leading edge and the side under pressure (Figure 13a) [37]. In the first 20 min, there was no ice on the tip of the coated blade, while the ice thickness on the tip of the uncoated blade was 6 mm. After 100 min, the ice on the coating was 9.6 mm thick, which was 40% thinner than that on the uncoated blade (Figure 13b). The hydrophobicity of the surface made the water droplets easily roll off the coating, and the low thermal conductivity of the silicone rubber reduced heat transfer, thus slowing or hindering ice formation [38]. Different from ice growth in an artificial climate chamber, the ice growth rate rose with time, which might have resulted from the decreasing temperature during the test time [39] (Figure 14). Due to the low affinity for ice on the hydrophobic surface, the ice can hardly form firm adhesion on the coating surface [40]. In addition, the separation pulses of the elastomer, the centrifugal force, and the vibrations generated by the rotation of wind turbine blades caused the ice to easily separate from the coatings [11,35]. After 238 min, the ice on the coating was shaken off, while the ice layer thickness on the uncoated blade reached up to 37 mm. The results indicate that the elastic coatings could keep the ice thickness within 30 mm (Figure 15). After 294 min, the ice on the uncoated blade was shaken off. This indicates that the ice on an uncoated blade might be thicker than 37 mm, and heavy ice remained on the uncoated blade for 1 h longer than it did on the coated blade. In summary, compared with the uncoated blade, the coated blade had three advantages: (1) a lagging freezing time, (2) lesser ice accumulation, and (3) a short icing/deicing cycle. Thus, the elastic deicing coatings could mitigate icing hazards and increase the output power of wind turbines.

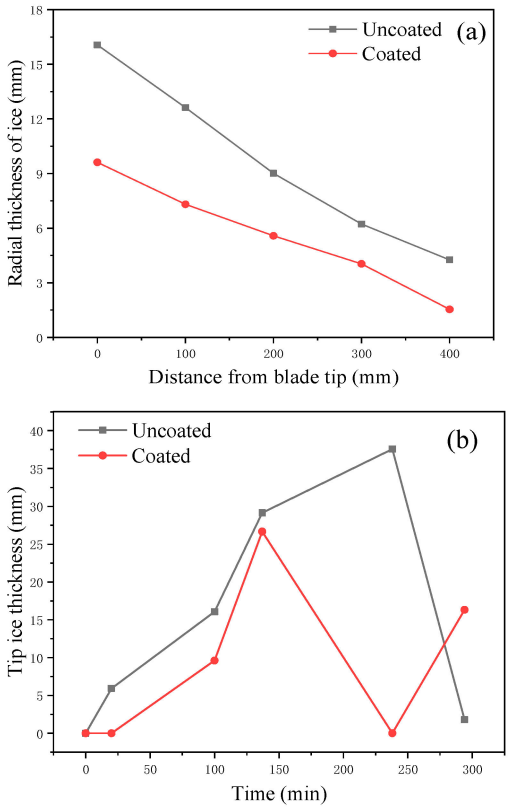

Figure 13. Ice thickness distribution on small wind turbine blades. (**a**) Ice thickness distribution on coated and uncoated blades. (**b**) Ice thickness changes over time.

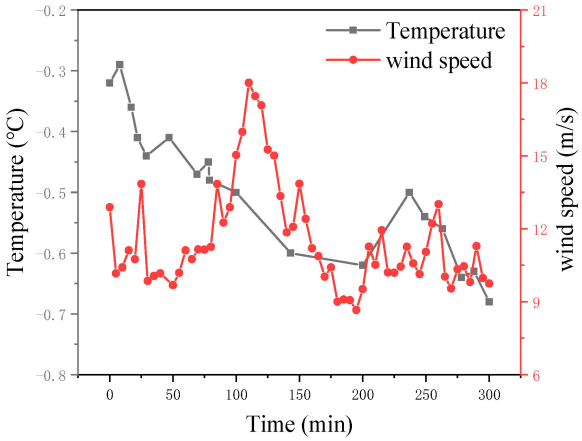

Figure 14. The temperature and speed changes during the dynamic deicing test.

Figure 15. Ice accumulation and distribution on the coated and uncoated small wind turbine blades.

4. Conclusions

Silicone rubber elastomer with a low ice adhesion strength has been identified as a potential anti-icing and deicing coating. In this study, elastic deicing coatings composed of silicone rubber and silica were developed with the aim of balancing icephobicity and mechanical properties, thus inhibiting ice adhesion and increasing durability simultaneously. The elastic deicing coating with 0.25% silica had the highest hydrophobicity and the lowest ice adhesion strength. Xenon lamp accelerated aging led to a decrease in hydrophobicity, which resulted from a decrease in the quantity of methyl groups in the coatings, an increase in surface roughness, and a decrease in the tensile modulus of the deicing coatings. Even though natural aging caused by insolation and wind erosion resulted in an increase in the ice adhesion strength and a decrease in the contact angle, the deicing coatings were still icephobic surfaces and had lower ice adhesion strength than the uncoated blade. Thus, the ice could easily be detached from the elastic deicing coatings, and the coatings kept the ice thickness at a low level. The present study verified the deicing performance of elastic deicing coatings and the feasibility of long-term operation on wind farms. However, the present work still cannot support the large-scale application of elastic deicing coatings; more work on operational wind turbines is needed.

Supplementary Materials: The following supporting information can be downloaded at: https://www.mdpi.com/article/10.3390/coatings14070870/s1, Figure S1: The SEM picture with different magnification of natural aging coatings; Figure S2: The wind fan used for the durability test of the elastic deicing coatings; Figure S3: Wind turbine used for dynamic deicing test; Figure S4: The picture used for ice thickness measurement.

Author Contributions: Conceptualization, data curation, writing, funding acquisition, K.L.; conceptualization, methodology, investigation, resources, writing, Z.X.; project administration, investigation, resources, D.J., Q.S. and J.L.; data curation, formal analysis, methodology, Z.C.; supervision, methodology, Y.Z. All authors have read and agreed to the published version of the manuscript.

Funding: This work was supported by the National Key R&D Program of China (Grant No. 2022YFB4100202) and basic research expenses from Zhejiang University of Science and Technology (2023QN004).

Institutional Review Board Statement: Not applicable.

Informed Consent Statement: Not applicable.

Data Availability Statement: Data are contained within the article.

Acknowledgments: Guangcheng Gu and Chonghui Jin of Guodian Ningbo Wind Power Development Co., Ltd. provided invaluable assistance in performing this wind turbine icing field study.

Conflicts of Interest: The authors Danqing Jiang, Qi Si, and Jixin Liu are employed by the company Guodian Ningbo Wind Power Development Co., Ltd. The remaining authors declare that this research was conducted in the absence of any commercial or financial relationships that could be construed as a potential conflict of interest.

References

1. Wei, K.; Yang, Y.; Zuo, H.; Zhong, D. A review on ice detection technology and ice elimination technology for wind turbine. *Wind Energy* **2020**, *23*, 433–457. [CrossRef]
2. Parent, O.; Ilinca, A. Anti-icing and de-icing techniques for wind turbines: Critical review. *Cold Reg. Sci. Technol.* **2011**, *65*, 88–96. [CrossRef]
3. Dalili, N.; Edrisy, A.; Carriveau, R. A review of surface engineering issues critical to wind turbine performance. *Renew. Sustain. Energy Rev.* **2009**, *13*, 428–438. [CrossRef]
4. Ma, L.; Zhang, Z.; Gao, L.; Hu, H. An exploratory study on using Slippery-Liquid-Infused-Porous-Surface (SLIPS) for wind turbine icing mitigation. *Renew. Energy* **2020**, *162*, 2344–2360. [CrossRef]
5. Meuler, A.J.; Smith, J.D.; Varanasi, K.K.; Mabry, J.M.; McKinley, G.H.; Cohen, R.E. Relationships between Water Wettability and Ice Adhesion. *ACS Appl. Mater. Interfaces* **2010**, *2*, 3100–3110. [CrossRef] [PubMed]
6. Irajizad, P.; Al-Bayati, A.; Eslami, B.; Shafquat, T.; Nazari, M.; Jafari, P.; Kashyap, V.; Masoudi, A.; Araya, D.; Ghasemi, H. Stress-localized durable icephobic surfaces. *Mater. Horiz.* **2019**, *6*, 758–766. [CrossRef]
7. Li, J.; Zhao, Y.; Hu, J.; Shu, L.; Shi, X. Anti-icing Performance of a Superhydrophobic PDMS/Modified Nano-silica Hybrid Coating for Insulators. *J. Adhes. Sci. Technol.* **2012**, *26*, 665–679. [CrossRef]
8. Zhuo, Y.; Hakonsen, V.; He, Z.; Xiao, S.; He, J.; Zhang, Z. Enhancing the Mechanical Durability of Icephobic Surfaces by Introducing Autonomous Self-Healing Function. *ACS Appl. Mater. Interfaces* **2018**, *10*, 11972–11978. [CrossRef] [PubMed]
9. Shamshiri, M.; Jafari, R.; Momen, G. Icephobic properties of aqueous self-lubricating coatings containing PEG–PDMS copolymers. *Prog. Org. Coat.* **2021**, *161*, 106466. [CrossRef]
10. He, Q.; He, W.; Zhang, F.; Zhao, Y.; Li, L.; Yang, X.; Zhang, F. Research Progress of Self-Cleaning, Anti-Icing, and Aging Test Technology of Composite Insulators. *Coatings* **2022**, *12*, 1224. [CrossRef]
11. Beemer, D.L.; Wang, W.; Kota, A.K. Durable gels with ultra-low adhesion to ice. *J. Mater. Chem. A* **2016**, *4*, 18253–18258. [CrossRef]
12. He, Z.; Xiao, S.; Gao, H.; He, J.; Zhang, Z. Multiscale crack initiator promoted super-low ice adhesion surfaces. *Soft Matter* **2017**, *13*, 6562–6568. [CrossRef] [PubMed]
13. Soz, C.K.; Yilgor, E.; Yilgor, I. Influence of the coating method on the formation of superhydrophobic silicone–urea surfaces modified with fumed silica nanoparticles. *Prog. Org. Coat.* **2015**, *84*, 143–152. [CrossRef]
14. Yilgor, E.; Soz, C.K.; Yilgor, I. Wetting behavior of superhydrophobic poly (methyl methacrylate). *Prog. Org. Coat.* **2018**, *125*, 530–536. [CrossRef]
15. Kim, J.H.; Kim, M.J.; Lee, B.; Chun, J.M.; Patil, V.; Kim, Y. Durable ice-lubricating surfaces based on polydimethylsiloxane embedded silicone oil infused silica aerogel. *Appl. Surf. Sci.* **2020**, *512*, 145728. [CrossRef]
16. Memon, H.; De Focatiis, D.S.A.; Choi, K.; Hou, X. Durability enhancement of low ice adhesion polymeric coatings. *Prog. Org. Coat.* **2021**, *151*, 106033. [CrossRef]
17. Wu, X.; Chen, Z. A mechanically robust transparent coating for anti-icing and self-cleaning applications. *J. Mater. Chem. A* **2018**, *6*, 16043–16052. [CrossRef]
18. Liu, J.; Wang, J.; Mazzola, L.; Memon, H.; Barman, T.; Turnbull, B.; Mingione, G.; Choi, K.; Hou, X. Development and evaluation of poly (dimethylsiloxane) based composite coatings for icephobic applications. *Surf. Coat. Technol.* **2018**, *349*, 980–985. [CrossRef]
19. Zhuo, Y.; Li, T.; Wang, F.; Hakonsen, V.; Xiao, S.; He, J.; Zhang, Z. An ultra- durable icephobic coating by a molecular pulley. *Soft Matter* **2019**, *15*, 3607–3611. [CrossRef]

20. Ronneberg, S.; He, J.; Zhang, Z. The need for standards in low ice adhesion surface research: A critical review. *J. Adhes. Sci. Technol.* **2020**, *34*, 319–347. [CrossRef]
21. Eshaghi, A.; Mesbahi, M.; Aghaei, A.A. Transparent hierarchical micro-nano structure PTFE-SiO_2 nanocomposite thin film with superhydrophobic, self-cleaning and anti-icing properties. *Optik* **2021**, *241*, 166967. [CrossRef]
22. Roach, P.; Shirtcliffe, N.J.; Newton, M.I. Progess in superhydrophobic surface development. *Soft Matter* **2008**, *4*, 224–240. [CrossRef] [PubMed]
23. Xie, Q.; Hao, T.; Zhang, J.; Wang, C.; Zhang, R.; Qi, H. Anti-Icing Performance of a Coating Based on Nano/Microsilica Particle-Filled Amino-Terminated PDMS-Modified Epoxy. *Coatings* **2019**, *9*, 771. [CrossRef]
24. Wong, T.; Kang, S.H.; Tang, S.K.Y.; Smythe, E.J.; Hatton, B.D.; Grinthal, A.; Aizenberg, J. Bioinspired self-repairing slippery surfaces with pressure-stable omniphobicity. *Nature* **2011**, *477*, 443–447. [CrossRef] [PubMed]
25. Golovin, K.; Kobaku, S.P.R.; Lee, D.H.; DiLoreto, E.T.; Mabry, J.M.; Tuteja, A. Designing durable icephobic surfaces. *Sci. Adv.* **2016**, *2*, e1501496. [CrossRef] [PubMed]
26. Xu, M.; Zhao, Y.; Zhang, X.; Li, Z.; Zhao, L.; Wang, Z.; Gao, W. Highly Homogeneous Polysiloxane Flexible Coating for Low Earth Orbital Spacecraft with Ultraefficient Atomic Oxygen Resistance and Self-Healing Behavior. *ACS Appl. Polym. Mater.* **2019**, *1*, 3253–3260. [CrossRef]
27. Liu, Y.; Ma, L.; Wang, W.; Kota, A.K.; Hu, H. An experimental study on soft PDMS materials for aircraft icing mitigation. *Appl. Surf. Sci.* **2018**, *447*, 599–609. [CrossRef]
28. Sobhani, S.; Bakhshandeh, E.; Jafari, R.; Momen, G. Mechanical properties, icephobicity, and durability assessment of HT-PDMS nanocomposites: Effectiveness of sol-gel silica precipitation content. *J. Sol-Gel Sci. Technol.* **2023**, *105*, 348–359. [CrossRef]
29. Illescas, J.F.; Mosquera, M.J. Surfactant-Synthesized PDMS/Silica Nanomaterials Improve Robustness and Stain Resistance of Carbonate Stone. *J. Phys. Chem. C* **2011**, *115*, 14624–14634. [CrossRef]
30. Xu, F.; Wang, C.; Li, D.; Wang, M.; Xu, F.; Deng, X. Preparation of modified epoxy-SiO_2 hybrid materials and their application in the stone protection. *Prog. Org. Coat.* **2015**, *81*, 58–65. [CrossRef]
31. Haddad, G.; Wong, K.L.; Petersen, P. Evaluation of the Aging Process of Composite Insulator based on Surface Charaterisation Techniques and Electrical Method. *IEEE Trans. Dielectr. Electr. Insul.* **2016**, *23*, 311–318. [CrossRef]
32. Zhang, Y.; Zhang, Z.; Jiang, X.; Liang, T.; Zhang, D. Research on Lifespan Prediction of Composite Insulators in a High Altitude Area Experimental Station. *Appl. Sci.* **2019**, *9*, 3364. [CrossRef]
33. Savadkoohi, E.M.; Mirzaie, M.; Seyyedbarzegar, S.; Mohammadi, M.; Khodsuz, M.; Pashakolae, M.G.; Ghadikolaei, M.B. Experimental investigation on composite insulators AC flashover performance with fan-shaped non-uniform pollution under electro-thermal stress. *Int. J. Electr. Power Energy Syst.* **2020**, *121*, 106142. [CrossRef]
34. Xi, B.; Zhao, T.; Gao, Q.; Wei, Z.; Zhao, S. Surface wettability effect on heat transfer across solid-water interfaces. *Chem. Eng. Sci.* **2022**, *254*, 117618. [CrossRef]
35. Liu, Z.; Zhang, Y.; Li, Y. Superhydrophobic coating for blade surface ice-phobic properties of wind turbines: A review. *Prog. Org. Coat.* **2024**, *187*, 108145. [CrossRef]
36. Hejazi, V.; Sobolev, K.; Nosonovsky, M. From superhydrophobicity to icephobicity: Forces and interaction analysis. *Sci. Rep.* **2013**, *3*, 2194. [CrossRef] [PubMed]
37. Gao, L.; Hu, H. Wind turbine icing characteristics and icing-induced power losses to utility-scale wind turbines. *Proc. Natl. Acad. Sci. USA* **2021**, *118*, e2111461118. [CrossRef] [PubMed]
38. Huang, W.; Huang, J.; Guo, Z.; Liu, W. Icephobic/anti-icing properties of superhydrophobic surfaces. *Adv. Colloid Interface Sci.* **2022**, *304*, 102658. [CrossRef] [PubMed]
39. Shu, L.; Liang, J.; Hu, Q.; Jiang, X.; Ren, X.; Qiu, G. Study on small wind turbine icing and its performance. *Cold Reg. Sci. Technol.* **2017**, *134*, 11–19. [CrossRef]
40. Wei, X.; Cai, F.; Wang, J. Electrothermal/photothermal superhydrophobic coatings based on micro/nano graphite flakes for efficient anti-icing and de-icing. *Prog. Org. Coat.* **2023**, *182*, 107696. [CrossRef]